Applied Catalysis B: Environmental 147 (2014) 293–301

Contents lists available at ScienceDirect

Applied Catalysis B: Environmental

journal homepage: www.elsevier.com/locate/apcatb

Biomass derived chemicals: Environmentally benign process for oxidation of 5-hydroxymethylfurfural to 2,5-diformylfuran by using nano-fibrous Ag-OMS-2-catalyst

Ganapati D. Yadav*, Rajesh V. Sharma

Department of Chemical Engineering, Institute of Chemical Technology, Nathalal Parekh Marg, Matunga, Mumbai 400 019, India

ARTICLE INFO

Article history:
Received 23 April 2013
Received in revised form 29 July 2013
Accepted 2 September 2013
Available online 8 September 2013

Keywords:
Biorefinery
Biomass
Green process
Oxidation
5-Hydroxymethylfurfural
2,5-Diformylfuran
Kinetics

ABSTRACT

5-Hydroxymethylfurfural (HMF) will be a major feedstock derived from waste/fresh biomass, which could be converted into a variety of valuable chemicals. The present work deals with an efficient, robust, environmentally benign and selective catalyst for preparation of 2,5-diformylfuran (DFF) from 5-hydroxymethylfurfural (HMF). It was investigated that impregnation of silver in K-OMS-2 (octahedral molecular sieve) improved the activity of the catalyst by decreasing concentration of acidic sites and increasing basic sites which was confirmed by NH_3 and CO_2-TPD results. Silver impregnation also decreases the reduction temperature of K-OMS-2 as confirmed by TPR study. HMF conversion and DFF selectivity were found to be 99 and 100%, respectively. Effects of various kinetic parameters on rate and conversion were studied. The reaction follows pseudo first order kinetics. The energy of activation is 11.54 kcal/mol. Product isolation protocol is discussed to obtain 99.9% of DFF purity. Ag-OMS-2 catalyst exhibits excellent reusability up to sixth run. Since the overall process is environmentally safe, catalyst is reusable and DFF yield is 99%, it is suitable for further industrial exploration.

1. Introduction

Biomass, both fresh and waste has been an important resource for the production of chemicals, fuels and energy. As compared to fuel, chemicals derived from biomass have great economic value and hence several routes have been proposed for the production of chemicals from biomass [1]. 5-Hydroxymethylfurfural (HMF) and furfural, which belong to the furan family and can be obtained from a variety of renewable carbohydrates, are building blocks of future bulk chemicals, fine chemicals and polymer industries. 5-Hydroxymethylfurfural (HMF) is considered as an important bridge molecule between biomass and specialty chemicals [2]. Selective oxidation of 5-hydroxymethylfurfural to 2,5-diformylfuran (DFF) is commercially important since it is a versatile compound. Its applications are varied and impressive such as: monomer [3–5], starting material for synthesis of pharmaceuticals [6], nematocides [7], antifungal agents [8], ligands, in photography as cross-linking agent for poly(vinyl alcohol), for battery separators, as foundry sand binders [9], for metal electroplating, in electro optical devices [10], as organic phosphors and luminophores and for preparing new polymeric materials for special applications [3,5,11]. Also it is used as starting material for the preparation of 2,5-bis(aminomethyl)-furan and Schiff bases [12].

Several reports are available on the preparation of DFF by oxidation of HMF using various classical, polluting and unsafe oxidants which must be used in stoichiometric amounts. Morikawa and Terakate [13] used the classical Swern oxidation as well as CrO_3-pyridine to convert HMF to DFF. Other oxidants include barium manganate [14], pyridinium chlorochromate (PCC), $Pb(OAc)_4$-pyridine, $K_2Cr_2O_7$-DMSO, 2,2,6,6-teramethylpiperidine-1-oxide (TEMPO) and trimethylammonium chlorochromate under ultrasonic conditions. Air oxidation of HMF catalyzed by homogeneous metal/bromide systems (Co/Mn/Br, Co/Mn/Zr/Br) is also reported [15]. However, the yields were attractive (57% isolated), coupled with the corrosive nature of the system which is a major disadvantage. A heterogeneous oxidation system such as titanium silicate (TS-1)/H_2O_2 has been employed to oxidize HMF in methanol or water. However, only 25% yield was observed [16]. Halliday et al. reported one pot preparation of DFF from fructose; however, the use of the solvent such as DMSO is deleterious, fraught with problems of solvent recovery and DFF purification. Moreover, low DFF yields were achieved, even at high catalyst ratio [17]. Moreau et al. performed the air oxidation of HMF in organic solvents such as toluene, benzene and methyl isobutyl ketone, using V_2O_5 alone or supported on TiO_2 and found HMF conversion between 30 and 90%,

* Corresponding author. Tel.: +91 22 3361 1001; fax: +91 22 3361 1002/1020.
E-mail addresses: gdyadav@yahoo.com, gd.yadav@ictmumbai.edu.in (G.D. Yadav).

0926-3373/$ – see front matter © 2013 Elsevier B.V. All rights reserved.
http://dx.doi.org/10.1016/j.apcatb.2013.09.004

Nomenclature

a	gas–liquid interfacial area/unit volume of liquid phase (cm^2/cm^3)
a_p	particle external surface area per unit liquid volume (cm^2/cm^3); $a_p = 6w/\rho_p d_p$
A	reactant species A, oxygen
A^*	concentration of A in reaction phase at gas–liquid interface (mol/cm^3)
$[A_S]$	concentration of A in reaction phase at exterior surface of catalyst particle (mol/cm^3)
B	reactant species B, HMF
$[B_0]$	concentration of B in bulk liquid phase, mol/cm^3
$[B_S]$	concentration of B at exterior surface of catalyst particle (mol/cm^3)
C	product species, DFF
C_{WP}	Wiesz–Prater criterion
D	product species D, water
D_A	diffusivity of A (cm^2/s)
$D_{A\text{-}e}$	effective diffusivity of A within catalyst pore space (cm^2/s)
k_G	gas-side mass transfer coefficient (cm/s)
$k_{G\text{-}A}a$	overall gas side mass transfer coefficient (s^{-1})
k_L	liquid-side mass transfer coefficient (cm/s)
$k_{L\text{-}A}a$	overall liquid side mass transfer coefficient (s^{-1})
$K_{L\text{-}A}$	overall mass transfer coefficient for transfer of gas (oxygen) from gas phase to bulk liquid phase (cm/s).
k_{SL}	solid–liquid mass transfer coefficient (cm/s)
$k_{SL\text{-}B}$	solid–liquid mass transfer coefficient for B (cm/s)
k_{SR}	kinetic rate constant (cm^3 /atm/s/g-cat^{-1})
k'_{SR}	combined rate constant (s^{-1})
M_A	overall mass transfer coefficient (s^{-1})
P_A	pressure of A (atm)
p_{O_2}	pressure of oxygen (atm)
R_A	rate of mass transfer of species A into liquid phase ($mol/(cm^3\ s)$)
$-r_B$	rate of reaction of B ($mol/(cm^3\ s)$)
R_B	rate of transfer of B (HMF) from bulk liquid phase to external surface of the catalyst particle ($mol/(cm^3\ s)$)
r_{obs}	observed rate of reaction based on liquid volume for specific catalyst loading ($mol/(cm^3\ s)$)
r_p	particle radius (cm)
Sh	Sherwood number $(k_{SL\text{-}B} \cdot d_p)/D_A$
t	time (s)
w	catalyst loading per unit liquid volume (g/cm^3)
W	water
X_B	fractional conversion of B

Greek letters

ε	fractional porosity of particle
ρ_p	particle density (g/cm^3)
τ	tortuiosity

with selectivity DFF of 90–60% [18]. Carlini et al. reported oxidation of HMF to DFF by using $VOPO_4{\cdot}2H_2O$ and, DMF as solvent, and selectivity of DFF up to 90% was achieved; however, HMF conversion was not satisfactory and quite low (20–56%) [19]. Mn(III)-salen catalyst was used for HMF oxidation with sodium hypochlorite at pH 11.3 to get 63–89% yield, but the reaction was sluggish taking more than 24 h [20]. Antonyraj et al. used Ru/γ-alumina catalyst and reported 99% HMF conversion. However; the catalyst is costly and also undergoes deactivation [1]. Takagaki et al. [21] used hydrotalcite supported ruthenium catalyst and obtained 92% yield of DFF in *N*,*N*-dimethylformamide solvent that made it difficult to isolate the product. Yang et al. [2] used K-OMS-2 catalyst and reported that OMS has good activity but found it applicable in the presence of pure oxygen [2]. Sadaba et al. [22] used zeolite supported vanadia and reported 84% of HMF conversion and 99% of DFF selectivity; however, the catalyst showed leaching of vanadium in the reaction media. So far, most of the reported catalysts either suffer with poor reusability and low DFF yield or are environmentally unsafe.

Scheme 1 shows the oxidation of HMF which involves a complex reaction mechanism and produces several products such as 2,5-diformylfuran (DFF), 5-hydroxymethyl-2-furancarboxylic acid (HMFCA), 5-formyl-2-furancarboxylic acid (FFCA), 2,5-furandicarboxylic acid (FDCA). Hence, design and preparation of a suitable catalyst for the selective formation of DFF is still a challenging task. The current work gives an insight into the oxidation of HMF to DFF over manganese oxide octahedral molecular sieves (K-OMS) and silver loaded OMS-2 as oxidizing catalysts by using air as oxidant. K-OMS-2 is a well known redox type of heterogeneous catalyst [23,24]. It was reported that K-OMS-2 is acidic in nature, and has an affinity for aldehydes which makes the catalyst non-reusable and less active [2]. Recently, our group investigated that incorporation of silver in K-OMS-2 renders a catalyst with lower acidity and increased basicity vis-à-vis pure K-OMS-2 [25]. Hence, it was hypothesized that a decrease in acidity and increase in basicity of the K-OMS-2 by incorporation of silver, can increase the activity of the catalyst, enhance selectivity of DFF, and can also improve the reusability of K-OMS-2-based catalyst. This is the first report for use of Ag-OMS-2 catalyst for selective oxidation of HMF to DFF in the presence of air. The role of polar and non-polar solvents was also investigated to influence selectivity.

2. Experimental

2.1. Chemicals

The following chemicals were procured from firms of repute and used without further purification: manganese acetate (AR), potassium permanganate (AR), silver nitrate (AR), nitric acid (AR), ethanol (LR), methanol (LR) and isopropyl alcohol (LR) (M/s S.D. Fine Chem. Ltd., Mumbai, India). Air (GC grade purity) was obtained in cylinders from Inox India Ltd., Mumbai.

2.2. Catalyst preparation

Silver substituted manganese oxide octahedral molecular sieve (Ag-OMS-2) was synthesized by precipitation method under acidic condition as discussed earlier [25–30].

2.3. Catalyst characterization

The synthesized catalysts were fully characterized by the following methods: Thermo-gravimetric Analysis (TGA), Scanning Electron Microscopy (SEM), X-ray Diffraction (XRD), Energy Dispersive X-ray Spectroscopy (EDXS), Temperature Programmed Desorption (TPD) and Temperature Programmed Reduction (TPR), surface area and pore volume using Brunauer–Emmett–Teller (BET) method. Details of conditions and equipment used are discussed in detail by Yadav and co-workers. [24–27,29,30]. The catalyst leaching study was carried out by ICP-MS. A 0.5 g of the reaction mixture was mixed with 2.0 g of concentrated hydrofluoric acid (48–51%). Then, the final solution was prepared by using 0.2 N HNO_3 acid and analyzed by a ICP-MS.

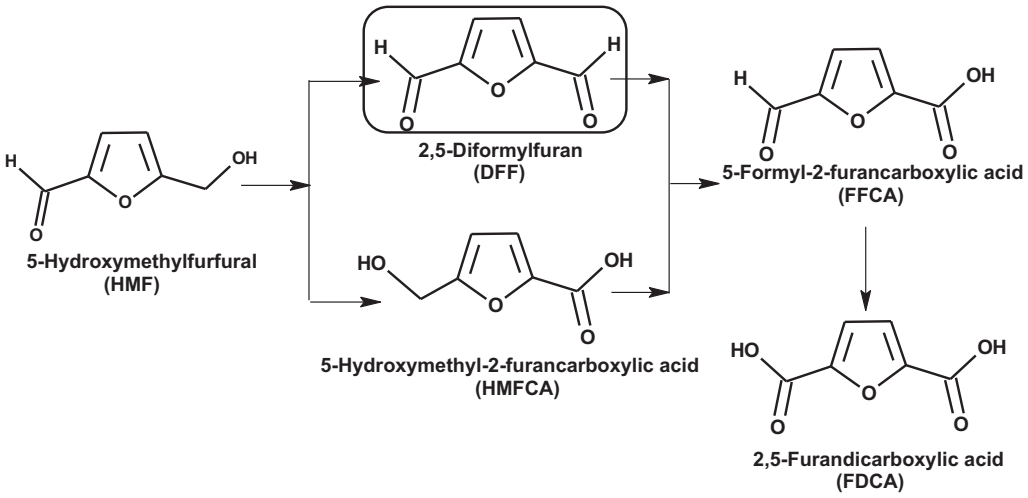

Scheme 1. Oxidation of 5-hydroxymethylfurfural (HMF) with air.

2.4. Reaction procedure

All experiments were carried out in a 100 cm^3 autoclave reactor made of Hastloy C supplied by Amar Autoclave, Mumbai, India. A four bladed pitch turbine impeller was used for agitation. The temperature was maintained at ±1 °C of the desired value by PID controller. The rector was equipped with gas inlet and outlet ports, sample port, rupture disk and a magnetic drive to vary the speed of agitation. Air cylinder was used along with a constant pressure regulator for supply of air. Before starting the reaction, the catalyst was dried for 2 h at 120 °C in an oven. The standard reaction was carried out by taking 0.0025 mol HMF, 40 cm^3 of solvent (isopropyl alcohol), catalyst loading was 0.0075 g/cm^3. Air was charged up to the required pressure at room temperature. Then heating was started. A zero time sample was withdrawn when the reaction mixture reached the desired reaction temperature to take care of any conversion during this temperature ramp because minimum 30 min was required to heat the reactor from room temperature to the reaction temperature. Thereafter, agitation was commenced at 1000 rpm and samples were withdrawn after fixed intervals of time and analyzed by HPLC. During the reaction, air pressure was maintained constant by a pressure regulator.

2.5. Method of analysis

Samples were analyzed by using a Knauer HPLC pump and RP-8 column, coupled to a Knauer UV detector (283 nm). The mobile phase was acetonitrile: water: acetic acid (60:39:1) with a flow rate of 0.5 cm^3/min. Authentic samples of HMF and DFF were used as standards, and calibration was done for quantitative analysis.

2.6. Product isolation procedure

After completion of the reaction, the reactor was cooled down. The catalyst was filtered and washed with isopropyl alcohol (10 $cm^3 \times 3$). The reaction mixture and washing were collected. Isopropyl alcohol was evaporated on a rotary evaporator to get pure DFF (purity 99.9% by HPLC). DFF was confirmed by mass, IR, NMR and GCMS.

3. Results and discussion

3.1. Catalyst characterization

Nano fibrous brownish black colored Ag-OMS-2 powder was obtained after calcination at 400 °C for 4 h. It was reported in literature that Ag-OMS-2 catalyst has a 1-D tunnel structure formed by 2 × 2 edge shared MnO_6 octahedral chains [27,28]. Ag-OMS-2 synthesis, and its complete catalyst characterization are reported by our group [25–27]. Hence, a brief discussion of catalyst characterization is described here relevant to the results obtained in this work. The catalyst stability was performed by TGA analysis and it showed that all catalysts were stable up to 500 °C. Fig. 1 shows the SEM images of (A) K-OMS-2 and (B) 15 wt% Ag-OMS-2 which confirmed the presence of the nano fibrous structure of the catalyst, and surface morphology of K-OMS-2 remained unaltered even after addition of silver in K-OMS-2. The presence of silver in catalyst was confirmed by EDX analysis. The basic cryptomelane structure of the catalyst and existence of silver ions in the catalyst was confirmed by XRD analysis [25].

Addition of silver in K-OMS-2 decreases the acidity of the catalyst and it also improves the redox properties of the catalyst which was confirmed by TPD and TPR study. Table 1 shows TPD analysis with ammonia and carbon dioxide as probe molecules. It also reveals the presence of acidic and basic sites on the surface of the catalyst. K-OMS-2 has the total acidity 339 μmol/g of ammonia adsorbed; however, 5, 10, 15 wt% of Ag-OMS-2 catalysts have 317, 234 and 230 μmol/g of ammonia adsorbed, respectively, showing decrease in acidity with increasing Ag incorporation. The CO_2-TPD results of K-OMS-2 and 5, 10, 15 wt% of Ag-OMS-2 show that with increase in silver loading increases the basicity of catalysts (see Table 1). The TPR studies of K-OMS-2, and 5, 10, 15 wt% of Ag-OMS-2 was carried out by using hydrogen as probe molecule. It was observed that the reduction temperature of the catalyst decreased from 280 to 160 °C with increase in silver loading in K-OMS-2 which is also in agreement with the literature reports [26,31,32]. The decrease in acidity and increase in basicity of K-OMS-2 catalyst by incorporation of silver can be due to the exchange of

Table 1
NH_3-TPD, CO_2-TPD and H_2-TPR studies: effect of Ag substitution.

Catalyst	NH_3 adsorbed μmol/g catalyst (140-200 °C)	CO_2 adsorbed μmol/g catalyst (100-140 °C)	H_2-TPR (°C)
K-OMS-2	339	216	280
5 wt%-Ag-OMS-2	317	309	190
10 wt%-Ag-OMS-2	309	372	170
15 wt%-Ag-OMS-2	230	374	160

Table 2
Effects of solvent.

Solvent	Conversion of HMF (%)	Selectivity of DFF (%)
Dimethyl sulfoxide	90	96
N,*N*-Dimethylformamide	78	95
Methanol	92	64
Ethanol	97	87
Isopropyl alcohol	99	100
Methyl isobutyl ketone	64	95
Toluene	60	96

Experimental conditions: 0.0025 mol of HMF, 0.0075 g/cm^3 (15 wt%-Ag-OMS-2) of catalyst, 1000 rpm, 15 atm of air, 240 min, 40 cm^3 of IPA, 165 °C.

Table 3
Effects of silver loading on K-OMS-2.

Catalyst	Conversion of HMF (%)	Selectivity of DFF (%)
k-OMS-2	62	82
5 wt% Ag-OMS-2	81	95
10 wt% Ag-OMS-2	90	99
15 wt% Ag-OMS-2	99	100

Experimental conditions: 0.0025 mol of HMF, 0.0075 g/cm^3 of catalyst, 1000 rpm, 15 atm of air, 240 min, 40 cm^3 of IPA, 165 °C.

potassium ions with silver ions. Basic sites are provided by Mn^{4+} ions. The decrease in reduction temperature from 280 to 160 °C of K-OMS-2 after incorporation of silver can be due to the hydrogen spill over effect of silver which is present in finely dispersed form in the catalyst which is confirmed by SEM analysis. It was observed that with increase in silver content the BET surface area (m^2/g) and BJH pore volume (cm^3) increased from (89.1, 0.463) for K-OMS in the following order: 5%-Ag-OMS-2 (100.1, 0.518), 10% Ag-OMS-2 (110.7, 0.589) and 15% Ag-OMS-2 (118.6, 0.659) which is also in accordance with the literature report [25]. Silver being smaller in size than potassium, the partial replacement leads to corresponding increase in surface area and pore size. It is also reported in the literature that incorporation of silver results in partial replacement of potassium ions from the channel which changes the catalytic properties due to silver–manganese interaction, and increases the surface properties [33,34].

3.2. Effects of solvent

It was observed that nature of solvent has a very significant influence on the conversion of HMF and selectivity of DFF. Table 2 shows a systematic study of various high boiling and polar solvents (such as DMSO and DMF), low boiling and polar solvents (such as ethanol, methanol and isopropyl alcohol), and non-polar solvents (such as toluene). It was found that HMF conversions in polar solvent were good as compared with non-polar solvents which can be due to solubility of oxygen in the polar solvents which is more as compared to non-polar solvents. Yang et al. [2] also reported that polar solvent like DMSO shows better HMF conversion and DFF selectivity as compared to non-polar solvent such as toluene. DMSO and DMF are high boiling polar solvents and it makes product isolation step expensive and tedious. Hence we selected low boiling polar solvents such methanol, ethanol and isopropyl alcohol. We found that DFF selectivity was the highest i.e. 100% in case of isopropyl alcohol which is less polar than methanol and ethanol. However, methanol and ethanol showed 64 and 87% DFF selectivity. Hence, further study was done by taking isopropyl alcohol as solvent.

3.3. Effects of silver loading on K-OMS-2

The synthesized catalysts such as K-OMS-2, 5% Ag-OMS-2, 10% Ag-OMS-2 and 15 wt% Ag-OMS-2 were used for the oxidation of HMF at a constant air pressure of 15 atm and isopropyl alcohol as the solvent (Table 3). It was observed that HMF conversion increased from 62 to 99% with increasing silver content in K-OMS-2. It was also observed that DFF selectivity increased from 82 to

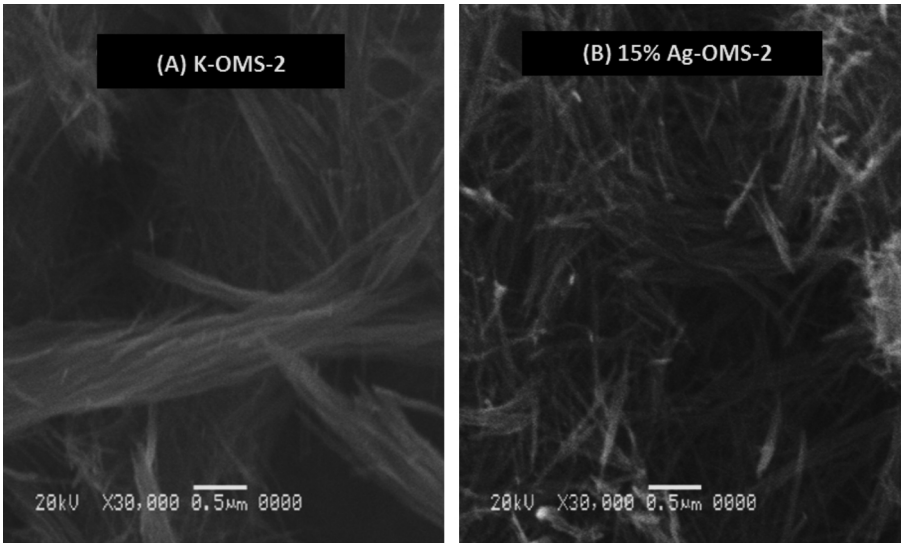

Fig. 1. SEM images of catalysts: (A) K-OMS-2, (B) 15 wt% Ag-OMS-2.

Table 4
Effects of speed of agitation.

Speed of agitation (rpm)	Conversion of HMF (%)	Selectivity of DFF (%)
600	81	100
800	90	100
1000	99	100
1200	99	100

Experimental conditions: 0.0025 mol of HMF, 0.0075 g/cm^3 (15 wt%-Ag-OMS-2) of catalyst, 600–1200 rpm, 15 atm of air, 240 min, 40 cm^3 of IPA, 165 °C.

100% with increased in silver content 5–15 wt% in K-OMS-2. The selectivity of DFF can be explained by NH_3-TPD results. It has been suggested [19,22] that surface acidity can promote HMF side reaction and lead to undesired products. Though, it was observed that the total acidity of the catalyst decreases with increase in silver content from 0 to 15 wt% in K-OMS-2 and hence, it is responsible for the increase in DFF selectivity. The increase in HMF conversion can be explained by TPR results. Yang et al. [2] reported that removal of secondary hydrogen is a rate determining step of HMF to produce DFF. The TPR studies showed that addition of silver reduces the reduction temperature of the K-OMS-2 catalyst from 280 to 160 °C. Hence the higher activity of Ag-OMS-2 can be contributed to its ability to remove the secondary hydrogen of HMF at a faster rate as compared to OMS-2. Hence, incorporation of silver in the framework of the catalyst improves activity and selectivity of the catalyst. 15 wt% Ag-OMS-2 showed the best results and hence it was selected for the further study.

3.4. Effects of speed of agitation

To study the influence of mass transfer resistance of the reactant molecules from the bulk liquid phase to the catalyst surface, the speed of agitation was varied in the range of 600–1200 rpm under otherwise similar experimental conditions. The mass transfer resistance in liquid film was evaluated by performing the reactions at four different speeds of agitation (600–1200 rpm). No significant increase in HMF conversion was observed beyond 1000 rpm (Table 4). Thus, further experiments were carried out at 1000 rpm. It ensured that there was no external mass transfer resistance during the reaction.

3.5. Proof of absence of external mass transfer and intra-particle diffusion resistance

This is a gas–liquid–solid (catalyst) slurry reaction, which has been analyzed adequately [35] to understand the role of external mass transfer resistance – gas to gas–liquid interface ($k_{G\text{-}A}a$), gas–liquid interface to bulk liquid phase ($k_{L\text{-}A}a$), and bulk liquid to solid exterior surface ($k_{SL\text{-}A}a_p$), where a is the gas–liquid interfacial area/unit volume of liquid phase (cm^2/cm^3), k_G, k_L and k_{SL} are gas-side, liquid-side and solid–liquid mass transfer coefficients (cm^2/s) for the respective species. The particle external surface area per unit liquid volume (cm^2/cm^3) is $a_p = 6w/\rho_p d_p$ where w is catalyst loading per unit liquid volume (g/cm^3), ρ_p particle density (g/cm^3) and dp particle diameter (cm).

The rate of mass transfer from oxygen from gas phase to the external surface of catalyst is given by:

$$R_A = M_A\,[[A^*] - [A_S]] \tag{1}$$

where the overall mass transfer coefficient

$$M_A = \left(\frac{1}{K_{L\text{-}A}a} + \frac{1}{k_{SL\text{-}A}a_p}\right)^{-1} \tag{2}$$

where $K_{L\text{-}A}$ is the overall mass transfer coefficient for transfer of gas (oxygen) from gas phase to liquid phase (cm^2/s).

Rate of transfer of B (HMF) from bulk liquid phase to external surface of the catalyst particle,

$$R_B = k_{SL\text{-}B}a_p\,[[B_0] - [B_S]] \tag{3}$$

$$R_B = R_A = r_{obs} \tag{4}$$

The stoichiometry of the reaction suggests the validity of Eq. (4) where the observed rate of reaction within the catalyst particle is, r_{obs}.

Here the subscripts "0" and "S" denote the concentrations in bulk liquid phase and external surface of catalyst, respectively. Depending on the relative magnitudes of the external resistance to mass transfer and reaction rates, different controlling mechanisms have been put forward and discussed [36] and different applications have been given to validate such theoretical analysis in some of our earlier work [37,38].

The effect of speed agitation showed that there was no mass transfer resistance for oxygen transfer from gas to external surface of the catalyst. This suggests that the concentration of dissolved oxygen on the external surface of catalyst was almost the same as its solubility in liquid phase at the operating pressure ($[A^*] = [A_S]$). The diffusivity of HMF in isopropanol was calculated from the Wilke–Chang equation [39] as 7.31×10^{-5} cm^2/s. The solid–liquid mass transfer co-efficient $k_{SL\text{-}B}$ for HMF was calculated from Sherwood number,

$$Sh = \frac{k_{SL-B}.d_p}{D_A} = 2 + 0.6Re_p^{1/2}Sc^{1/3} \quad \text{as} \quad 3.21 \times 10^{-2}\ \text{cm/s}.$$

where Re_p is the Reynolds number based on particle diameter and Sc is the Schmidt number. For a given concentration of HMF in the bulk liquid phase, there was no resistance to transfer of HMF from the bulk to the external surface of catalyst particle. So $[B_0] = [B_S]$. A typical calculation, the mass transfer transfer rate of HMF obtained was 2.31×10^{-5} mol/cm^2 s. The initial observed reaction rate was found to be 2.45×10^{-7} mol/cm^2 s. The mass transfer rate is higher than the overall reaction rate and hence, no influence of internal mass transfer resistance on reaction rate at 1000 rpm.

Wiesz–Prater criterion (C_{WP}), was invoked to assess the influence of intra-particle diffusion resistance. It is the ratio of the intrinsic reaction rate to intra-particle diffusion rate for a given particle radius (r_p), effective diffusivity of the limiting reactant (D_e) and concentration of the reactant at the external surface of the particle. If $C_{WP} = r_{obs}\rho_p r_p^2/D_e[A_S] \gg 1$, then the reaction is limited by severe internal diffusion resistance whereas $C_{WP} \ll 1$, then the reaction is intrinsically kinetically controlled.

The effective diffusivity of HMF ($D_{A\text{-}e}$) inside the pores of the catalyst was obtained from the bulk diffusivity (D_{AB}), porosity (ε) and tortuosity (τ), 7.95×10^{-5} cm^2/s where $D_{e\text{-}A} = D_{AB}\,(\varepsilon/\tau)$. The average value of porosity and tortuosity were taken as 0.4 and 3, respectively, as conservative estimate. In the present case, the value of C_{WP} was calculated as 1.51×10^{-3} which is much less than 1, which signifies the absence of resistance due to intra-particle diffusion and the reaction could be considered as an intrinsically kinetically controlled reaction. A further proof of the absence of the intra-particle diffusion resistance was obtained by the study of the effects of temperature, which will be discussed later.

3.6. Effect of air pressure

Effect of air pressure on HMF conversion and DFF selectivity was studied in the range of 10–25 atm (Fig. 2). It was observed that with the increase in air pressure from 10 to 15 atm, HMF conversion increased. Thereafter, from 15 to 25 atm the increase in HMF conversion was moderate. Selectivity of DFF in all cases remained almost 100%. Hence, all further experiments were carried out at air pressure 15 atm. The initial rate was plotted against the partial

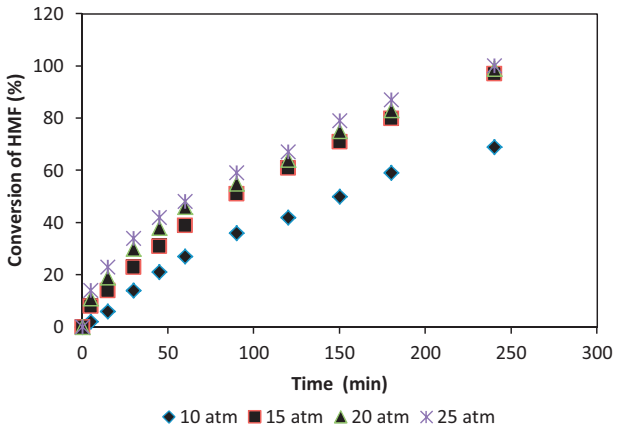

Fig. 2. Effect of air pressure on coversion of HMF 0.0025 mol of HMF, 0.0075 g/cm^3 of catalyst (15 wt% Ag-OMS-2), 1000 rpm, 10–25 atm of air, 240 min, 40 cm^3 of IPA, 165 °C.

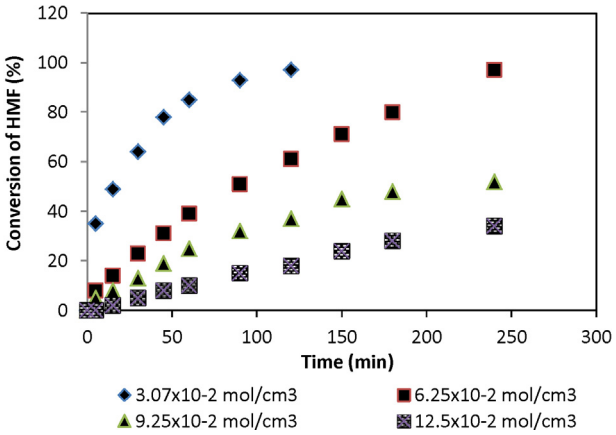

Fig. 4. Effect of concentration of HMF 3.07 × 10^{-2} to 12.5 × 10^{-2} mol/cm^3 of HMF, 0.0075 g/cm^3 of catalyst (15 wt% Ag-OMS-2), 1000 rpm, 15 atm of air, 240 min, 40 cm^3 of IPA, 165 °C.

pressure of oxygen ($P_A = p_{O_2}$). The rate of reaction is linear in p_{O_2} (Figure not shown). This is due to the increase in the solubility of oxygen in the reaction mass with pressure which is linear.

3.7. Effects of catalyst loading

The effect of catalyst loading was varied over the range of 0.005–0.01 g/cm^3 on the basis of total volume of the reaction mixture (Fig. 3). Conversion of HMF was found to increase with increase in catalyst loading. This increase in HMF conversion is due to a proportional increase in catalyst active sites due to increase in catalyst loading, which also demonstrates absence of both external mass transfer and intraparticle resistances. A reaction without catalyst reaction was also performed under otherwise similar reaction condition and, no conversion was observed. Further experiments were performed by taking 0.0075 g/cm^3 of 15 wt% Ag-OMS-2 catalyst. The initial rate was plotted against catalyst loading (figure is not shown). This also shows the rate is linear in catalyst loading.

3.8. Effects of concentration of HMF

The effects of concentration of HMF were studied at 3.07 × 10^{-2}, 6.25 × 10^{-2}, 9.25 × 10^{-2} and 12.5 × 10^{-2} mol/cm^3 by keeping similar experimental conditions. Conversion of HMF was found to decrease with increased in HMF concentration (Fig. 4). The initial rate of reaction increased linearly with initial concentration suggesting first order dependence. Selectivity of DFF was found to be 100% in all the cases. All further experiments were carried out by keeping 6.25 × 10^{-2} mol/cm^3 of HMF.

3.9. Effects of temperature

The reaction was carried out at 135, 145, 155 and 165 °C under otherwise similar experimental conditions (Fig. 5). It was observed that conversion increased with increase in temperature. At 165 °C, the conversion of HMF was 99% with 100% selectivity for 4 h. It suggested an intrinsically kinetically controlled mechanism as will be discussed later.

3.10. Catalyst stability and reuse

To examine leaching of active metal would occur or not, the HMF oxidation reaction was carried out for 1 h and then the reaction mixture was cooled to room temperature. Excess air was vented off and the catalyst was filtered from the reaction mixture. The reaction was carried out further without any catalyst. The HMF conversions after 4 h reaction time showed that there was no change in concentration of HMF without the catalyst. It confirmed that there was no leaching of active metal during the reaction. The ICP-MS analysis was also done and the liquid phase samples of the reaction mixture were tested for the presence of metal ions in a reaction

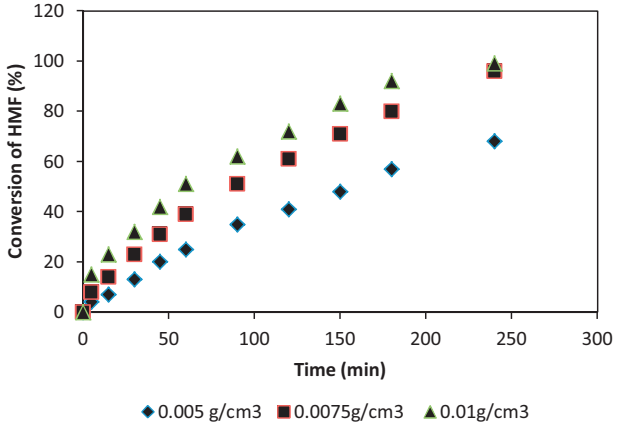

Fig. 3. Effects of catalyst loading on conversion of HMF: 0.0025 mol of HMF, 0.005–0.01 g/cm^3 of catalyst (15 wt% Ag-OMS-2), 1000 rpm, 15 atm of air, 240 min, 40 cm^3 of IPA, 165 °C.

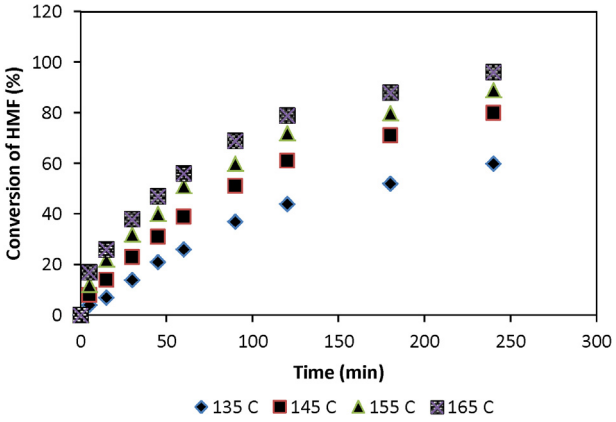

Fig. 5. Effect of temperature on conversion of HMF: 0.0025 mol of HMF, 0.0075 g/cm^3 of catalyst (15 wt% Ag-OMS-2), 1000 rpm, 15 atm of air, 240 min, 40 cm^3 of IPA, 135–165 °C.

Table 5
Catalyst reusability study.

Catalyst reused	Conversion of HMF (%)	Selectivity of DFF (%)
1st run	99	100
2nd run	98	100
3rd run	98	100
4th run	97	100
5th run	98	100
6th run	97	100

Experimental conditions: 0.0025 mol of HMF, 0.0075 g/cm^3 (15 wt%-Ag-OMS-2) of catalyst, 1000 rpm, 15 atm of air, 240 min, 40 cm^3 of IPA, 165 °C.

mixture after 1, 2 and 4 h. There was no presence of the metal ions detected.

The reusability of the catalyst was tested by conducting six runs (Table 5). After each experiment the catalyst was filtered and refluxed in 50 cm^3 of acetone for 30 min, to remove any adsorbed material from the catalyst surface and pores, and then recalcination was done at 350 °C for 3 h. Yang et al. [2] reported that aldehydes have an affinity for K-OMS-2 based catalyst and hence, it is adsorbed on catalyst surface and reduces the catalytic activity [2]. Only 81% HMF conversion was obtained after first run if catalyst was not recalcined at 350 °C. The recalcination of catalyst not only removed the DFF from catalyst surface but also oxidized unconverted Ag^+ to Ag^{2+} and Mn^{3+} to Mn^{4+} (see Scheme 2).

In a batch reaction, there are inevitable losses of particles during filtration. Hence, the actual amount of catalyst used in the next batch, was ~5% less than the previous batch. The loss of the catalyst was made up with fresh catalyst. The HMF conversion and DFF selectivity were found to be similar even after the 6th run. There was no reduction in selectivity of the catalyst which would mean that no catalyst active sites were changed. It has been also reported that K-OMS-2 is a redox catalyst and shows very fast oxidation and reduction cycle of the changing Mn^{4+} to Mn^{2+} and vice versa under given reaction conditions [27]. The substitution of K^+ with Ag^+ metal ions in K-OMS-2 framework also provides the robustness to K-OMS-2 [25]. Therefore, It can be concluded that 15 wt% Ag-OMS-2 catalyst is robust, reusable and economical for industrial exploration.

3.11. Plausible reaction mechanism

Octahedral molecular sieves (K-OMS-2) belong to a group of cryptomelane-type manganese oxide (MnO_6) having 1-dimensional 2 × 2 tunnel like structure with mixed valencies of manganese (such as Mn^{2+}, Mn^{3+}, and Mn^{4+}), which make it a good redox type of heterogeneous catalyst. The K^+ cations present in the tunnel act as active sites for selective catalytic reaction, and also help in balancing the charge of manganese [41]. Addition of silver in the catalyst exchanges the K^+ cation from the catalyst framework and decreases the reduction potential of the catalyst from 280 to 160 °C due to hydrogen spill over effect of silver. Silver is smaller in size than potassium and hence surface area and pore size increase. It was also observed that addition of silver not only reduced strong acidic sites of the catalyst to mild acidic sites but also increases the basicity of the catalyst (see Table 1). Further, it increases surface area since Ag^+ is smaller in size than K^+. The Ag-OMS-2 catalyst shows two different ammonia desorption peaks at lower temperature which is due to the presence of two different types of acidic sites one correspond to Ag^+ and another Mn^{4+} which is in accordance with the literature [25]. However, only one peak was seen in H_2-TPD confirms the redox nature of Ag-OMS-2.

Participation of lattice oxygen from the surface of K-OMS-2 during the oxidation reaction was suggested and proved by Suib and coworkers [41,42]. Mars–van Krevelen mechanism involves the participation of surface oxygen in the reaction and subsequently surface is regenerated with the oxygen supply source like air or oxygen. A redox mechanism was proposed for K-OMS-2 catalyzed HMF conversion to DFF by Yang et al. [2]. Based on this mechanism, a suitable model is derived from liquid phase air oxidation of HMF to DFF (Scheme 2). The oxidation reaction is initiated by conversion of Ag^{2+} into more stable Ag^+ ion and releases oxygen atom. Further, Mn^{3+} picks up the oxygen atom and get converted into Mn^{4+}. Steps 3 and 4 are based on reduction of Mn^{4+} to Mn^{3+} ion, and simultaneous oxidation of HMF to DFF. Steps 5 and 6 deal with catalyst regeneration steps whereas Mn^{3+} is oxidized to Mn^{4+} and Ag^+ is oxidized to Ag^{2+} [2,40]. Hence, the present study shows that the synergistic effects of silver and manganese in the OMS-2 are responsible for higher catalytic activity.

The reaction in the presence of 15 wt%-Ag-OMS-2 gives only DFF as a sole product with 100% selectivity.

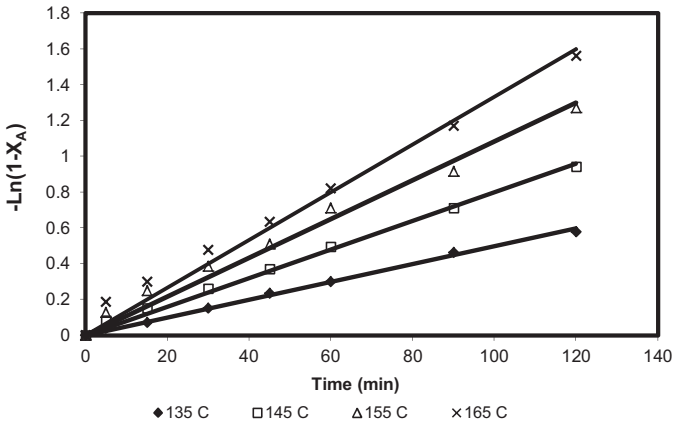

Fig. 6. Plot of $-\ln(1-X_B)$ vs. time at different temperatures.

3.12. Kinetic model

It is heterogeneous reaction and hence follows adsorption, surface reaction and desorption steps. The generalized schematic mechanism is shown in Scheme 3 which is based on Mars van Krevelin mechanism [40–43].

It is assumed that both molecules, HMF and oxygen, are adsorbed on actives sites. Oxygen adsorption takes place as a molecule rather than an atom through dissociative adsorption. Adsorbed species undergoes a surface reaction and produces DFF and water as a product. Product profile confirmed that reactant and products are weakly adsorbed on the surface and get desorbed very fast. Weak adsorption and desorption results in very high selectivity toward DFF.

If the surface reaction is a rate controlling step during above reaction with weak adsorption of all species, then the rate of reaction is given by:

$$-r_B = \frac{-d[B]}{dt} = k_{SR} w P_A [B] = [B_0] \frac{dX_B}{dt} = k_{SR} w P_A [B_0](1 - X_B)$$

Above equation suggests that rate of HMF oxidation under constant air pressure is a function of concentration of HMF only. By integrating the above equation leads to the following:

$$-\ln(1 - X_B) = k_{SR} w P_A t = k'_{SR} t$$

A plot of $-\ln(1-X_B)$ vs. time shows straight lines for all temperatures (Fig. 6). The model fits well for 135 and 145 °C with correlation coefficient $R^2 > 099$. However, at higher temperature of 155 and

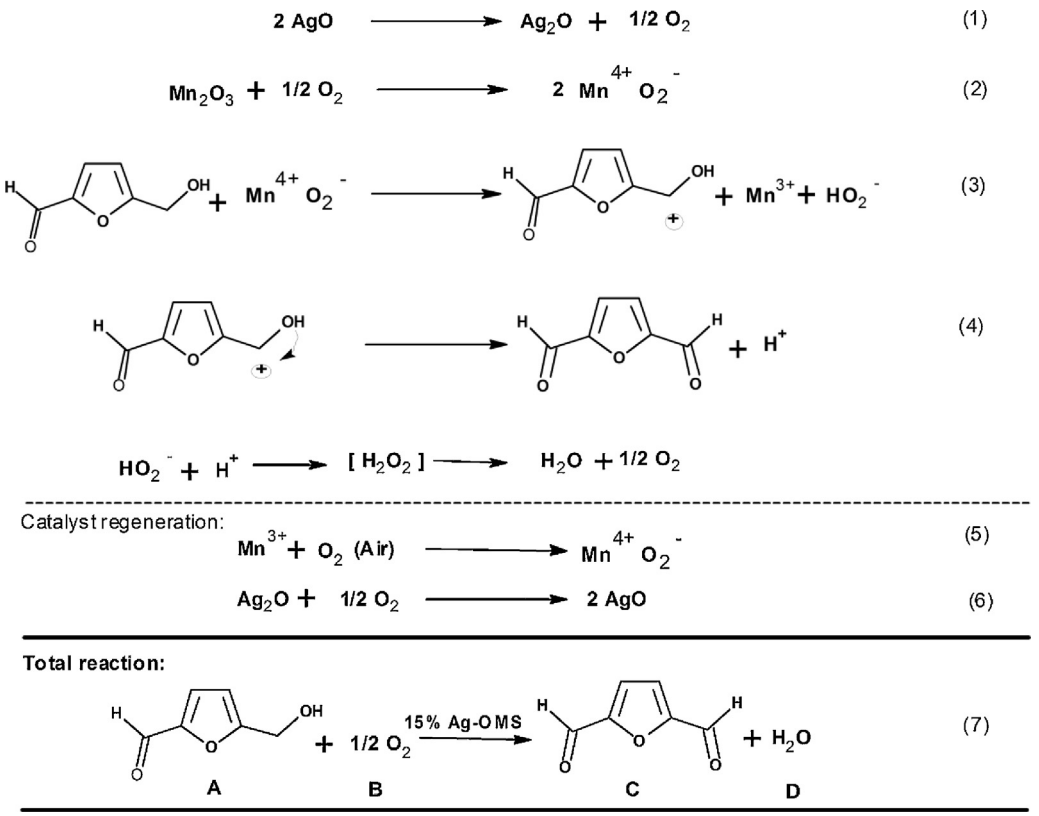

Scheme 2. Possible stepwise reaction mechanism over 15 wt% Ag-OMS-2 catalyst.

165 °C there is a deviation of initial data points from the straight line which is reflected in lower R^2 (0.97), when all points are considered which is due to very high initial rate of reaction. Since the reaction is kinetically controlled the rate is very high at higher temperatures. If only initial rate data points are used, then the correlation coefficient is improved. In order to have a better representation, all data points were considered with deviation of initial data points from the (pseudo-first order kinetic) line. Therefore, it confirms that the reaction is first order with respect to HMF.

Rate constants were calculated from Fig. 6 at different temperatures and Arrhenius plot made (Fig. 7). The value of apparent activation energy is 11.54 kcal/mol, which also suggests that the reaction is intrinsically kinetically controlled.

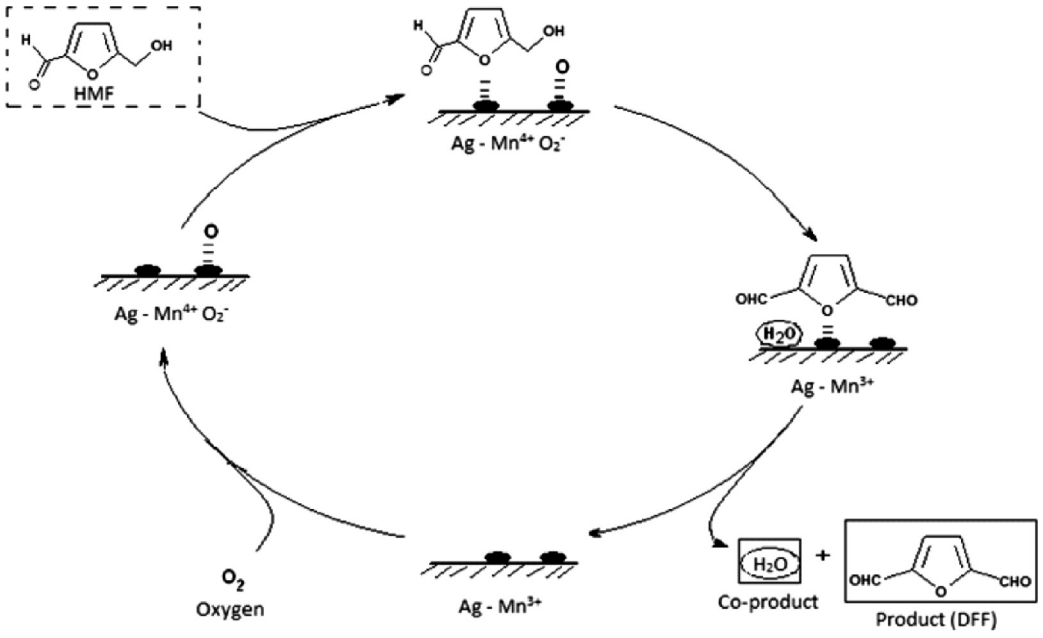

Scheme 3. Mars–van Krevelen mechanism over 15 wt% Ag-OMS-2 catalyst.

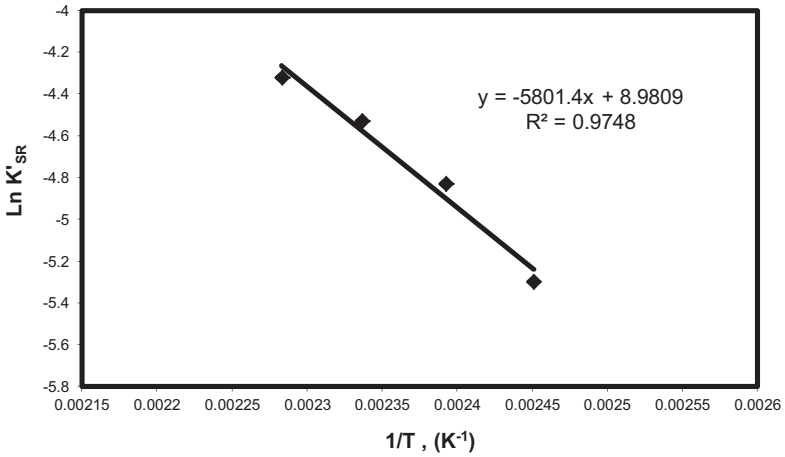

Fig. 7. Arrhenius plot.

4. Conclusions

In the present work, a simple and convenient oxidation process to convert HMF to DFF was developed. The catalyst is based on OMS-2 where K^+ is substituted by Ag^+. The effect of Ag substitution in K-OMS-2 was systematically studied which would give high conversion of HMF and excellent selectivity of DFF. Full catalyst characterization was done to understand the mechanism and to throw light on product formation. The TPR studies showed that addition of silver reduces the reduction temperature of K-OMS-2 from 280 to 160 °C. Hence, higher activity of Ag-OMS-2 can be contributed to its ability to remove the secondary hydrogen of HMF at a faster rate as compared to K-OMS-2. Incorporation of silver into the framework of OMS-2 improves the activity of the catalyst. The acidity of the catalyst is responsible for side reaction of HMF and it could be controlled through incorporation of silver in K-OMS-2 which decreases the acidity as confirmed by TPD analysis, and therefore selectivity to DFF increased. The effect of various solvents was also studied. The use of low boiling IPA made the product isolation easy. A yield of 99% of DFF with 99.9% of purity could be isolated. Effect of various parameters has been studied to establish that it is Mars van Krevelin type of mechanism. The reaction follows a pseudo first order kinetics. The HMF conversion and DFF selectivity were found to be similar even after the 6th run. Thus, 15 wt% Ag-OMS-2 is environmentally safe, robust and highly reusable catalyst. The value of apparent energy of activation is 11.54 kcal/mol. To our knowledge, no process is available on industrial scale to produce DFF from HMF. DFF is a very valuable chemical. Thus, this process has a potential for industrial exploitation.

Conflict of interest statement

The authors declare no conflict of interest.

Acknowledgment

This research was supported by CSIR-NMITLI program under the project on “Bioglycerol based chemicals”. G.D.Y. received support from R.T. Mody Distinguished Professor Endowment, and J.C. Bose National Fellowship of DST, Govt. of India. R.V.S. received JRF under this project.

References

[1] C.A. Antonyraj, J. Jeong, B. Kim, S. Shin, S. Kim, K.-Y. Lee, J.K. Cho, J. Ind. Eng. Chem. 19 (2013) 1056–1059.
[2] Z.-Z. Yang, J. Deng, T. Pan, Q.-X. Guo, Y. Fu, Green Chem. 14 (2012) 2986–2989.
[3] A. Gandini, M.N. Belgacem, Prog. Polym. Sci. 22 (1997) 1203–1379.
[4] A. Gandini, M.N. Belgacem, Polym. Int. 47 (1998) 267–276.
[5] A. Corma, S. Iborra, A. Velty, Chem. Rev. 107 (2007) 2411–2502.
[6] K.T. Hopkins, W.D. Wilson, B.C. Bender, D.R. McCurdy, J.E. Hall, R.R. Tidwell, A. Kumar, D.W. Boykin, J. Med. Chem. 41 (1998) 3872–3878.
[7] Rodriguez-Kabana, WO0067577, 2000.
[8] M.D. Poeta, W.A. Schell, C.C. Dykstra, S. Jones, R.R. Tidwell, A. Czarny, M. Bajic, A. Kumar, D. Boykin, J.R. Perfect, Antimicrob. Agents Chemother. 42 (1998) 2495–2502.
[9] H.C. Anderson, U.S. Patent 4,320,043, 1982.
[10] J. Daub, K.M. Rapp, P., Seitz, R., Wild, J. Salbeck, U.S. Patent 5,091,538, 1992.
[11] D. Hartzler, U.S. Patent 4,012,313, 1977.
[12] C. Moreau, M.N. Belgacem, A. Gandini, Top. Catal. 27 (2004) 1–4.
[13] S. Morikawa, S. Terakate, Japan Patent 7909260, 1979.
[14] T. El-Hajj, J.C. Martin, G. Descotes, J. Heterocycl. Chem. 20 (1983) 233–235.
[15] W. Partenheimer, V.V. Grushin, Adv. Synth. Catal. 343 (2001) 102–111.
[16] R.A. Sheldon, Stud. Surf. Sci. Catal. 59 (1991) 33–54.
[17] G.A. Halliday, R.J. Young Jr., V.V. Grushin, Org. Lett. 5 (2003) 2003–2005.
[18] C. Moreau, R. Durand, C. Pourcheron, D. Tichit, Stud. Surf. Sci. Catal. 108 (1997) 399–406.
[19] C. Carlini, P. Patrono, A.M.R. Galletti, G. Sbrana, V. Zima, Appl. Catal. A 289 (2005) 197–204.
[20] A.S. Amarasekara, D. Green, E. McMillan, Catal. Commun. 9 (2008) 286–288.
[21] A. Takagaki, M. Takahashi, S. Nishimura, K. Ebitani, ACS Catal. 1 (2011) 1562–1565.
[22] I. Sadaba, Y.Y. Gorbanev, S. Kegnaes, S.S.R. Putluru, R.W. Berg, A. Riisager, ChemCatChem. 5 (2013) 284–293.
[23] Z.R. Tian, J.Y. Wang, N.G. Duan, V.V. Krishnan, S.L. Suib, Science 276 (1997) 926–930.
[24] G.D. Yadav, H.G. Manyar, Adv. Synth. Catal. 350 (2008) 2286–2294.
[25] G.D. Yadav, R.K. Mewada, Chem. Eng. Res. Des. 90 (2012) 86–97.
[26] G.D. Yadav, R.K. Mewada, Chem. Eng. J. 221 (2013) 500–511.
[27] G.D. Yadav, R.K. Mewada, Catal. Today 198 (2012) 330–337.
[28] Y. Ding, X. Shen, S. Sithambaram, S. Gomez, R. Kumar, V.M.B. Crisostomo, S.L. Suib, M. Aindow, Chem. Mater. 17 (2005) 5382–5389.
[29] G.D. Yadav, R.V. Sharma. Indian Patent application number 3246MUM, 2010.
[30] G.D. Yadav, R.V. Sharma PCT application number PCTIN2011000061, 2011.
[31] M.J. Ramos, V. Jimenez, A. Funez, A. Romero, P. Sanchez, J.L. Valverde, Catal. Lett. 125 (2008) 220–228.
[32] Q. Fu, S. Kudriavtseva, H. Saltsburg, M.F. Stephanopoulos, Chem. Eng. J. 93 (2008) 41–53.
[33] W. Gac, Appl. Catal. B 75 (2007) 107–117.
[34] W. Gac, G. Giecko, S. Pasieczna-Patkowska, T. Borowiecki, L. Kepinski, Catal. Today 137 (2008) 397–402.
[35] P.A. Ramachandran, R.V. Chaudhari, Three-Phase Catalytic Reactors, Gordon and Breach Science Publishers, New York, 1983.
[36] G.D. Yadav, M.S. Krishnan, Ind. Eng. Chem. Res 37 (1998) 3358–3365.
[37] G.D. Yadav, S. Sengupta, Org. Process Res. Dev. 6 (2002) 256–262.
[38] G.D. Yadav, N.S. Doshi, Catal. Today 60 (2000) 263–273.
[39] R.C. Reid, M.J. Prausnitz, T.K. Sherwood, The Properties of Gases and Liquids, third ed., McGraw-Hill, New York, 1977.
[40] Y.S. Ding, X.F. Shen, S. Sithambaram, S. Gomez, R. Kumar, V.M.B. Crisostomo, S.L. Suib, M. Aindow, Chem. Mater. 17 (2005) 5382–5389.
[41] V.D. Makwana, Y.C. Son, A.R. Howell, S.L. Suib, J. Catal. 210 (2002) 46–52.
[42] Y.C. Son, V.D. Makwana, A.R. Howell, S.L. Suib, Angew. Chem. Int. Ed. 40 (2001) 4280–4283.
[43] G. Qiu, H. Huang, S. Dharmarathna, E. Benbow, L. Stafford, S.L. Suib, Chem. Mater. 23 (2011) 3892–3901.